ACS Sustainable Chemistry & Engineering

pubs.acs.org/journal/ascecg

Research Article

Lignin: A Sustainable Antiviral Coating Material

Alice Boarino,[#] Heyun Wang,[#] Francesca Olgiati, Fiora Artusio, Melis Özkan, Stefania Bertella, Nicolò Razza, Valeria Cagno, Jeremy S. Luterbacher, Harm-Anton Klok,[*] and Francesco Stellacci[*]

Cite This: *ACS Sustainable Chem. Eng.* 2022, 10, 14001−14010

Read Online

ACCESS | Metrics & More | Article Recommendations | Supporting Information

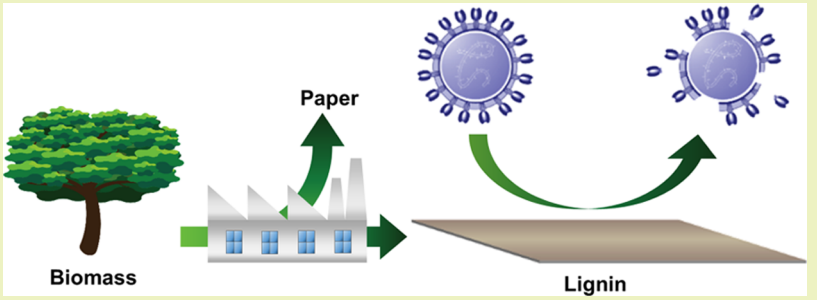

ABSTRACT: Transmission of viruses through contact with contaminated surfaces is an important pathway for the spread of infections. Antiviral surface coatings are useful to minimize such risks. Current state-of-the-art approaches toward antiviral surface coatings either involve metal-based materials or complex synthetic polymers. These approaches, however, even if successful, will have to face great challenges when it comes to large-scale applications and their environmental sustainability. Here, an antiviral surface coating was prepared by spin-coating lignin, a natural biomass residue of the paper production industry. We show effective inactivation of herpes simplex virus type 2 (>99% after 30 min) on a surface coating that is low-cost and environmentally sustainable. The antiviral mechanism of the lignin surface was investigated and is attributed to reactive oxygen species generated upon oxidation of lignin phenols. This mechanism does not consume the surface coating (as opposed to the release of a specific antiviral agent) and does not require regeneration. The coating is stable in ambient conditions, as demonstrated in a 6 month aging study that did not reveal any decrease in antiviral activity. This research suggests that natural compounds may be used for the development of affordable and sustainable antiviral coatings.

KEYWORDS: *lignocellulosic biomass, antiviral surface, sustainable material, herpes simplex virus type 2, reactive oxygen species*

INTRODUCTION

The COVID-19 outbreak illustrates the importance of technologies and measures against viral transmission in the environment.[1−4] Typical modes of viral transmission are airborne, waterborne, and fomite-mediated transmission. Airborne transmission involves infectious aerosols and droplet nuclei of viral particles, which is the most important infection pathway for respiratory viruses such as influenza virus and severe acute respiratory syndrome coronavirus (SARS-CoV, SARS-CoV-2).[5] Waterborne transmission is caused by the consumption of virus-contaminated water.[6] Fomite-mediated transmission, or contact transmission, mainly involves contact with virus-contaminated surfaces and has been considered to be an important route for viral transmission.[7−9] Many viruses, including, for example, norovirus and hepatitis virus, can persist on surfaces for up to 30−60 days and can lead to large outbreaks.[10,11]

Traditional measures against the aforementioned viral transmission routes include air/water filtration, decontamination by chemical disinfectants, heat inactivation, and ultraviolet light (UV) irradiation.[12,13] Although those measures are especially useful in inhibiting airborne and waterborne viral transmission, they are quite limited in disinfecting contaminated surfaces, which may potentially cause fomite-mediated transmission. The biggest limitation is that surfaces, unlike air or water, cannot be continuously disinfected, and frequent disinfection of surfaces is labor-intensive and is not realistic in most cases. Disinfection of contaminated surfaces can be avoided using materials or surface coatings that inactivate viruses.

To date, a number of antiviral surfaces have been developed to address the challenge of preventing fomite-mediated viral transmission. Typical materials for antiviral surfaces are quaternary ammonium compounds (QACs), metals and metal oxides (Cu, Ag, and TiO_2), and organic photosensitizers

Received: July 18, 2022
Revised: September 30, 2022
Published: October 13, 2022

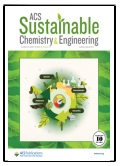

© 2022 The Authors. Published by American Chemical Society

https://doi.org/10.1021/acssuschemeng.2c04284
ACS Sustainable Chem. Eng. 2022, 10, 14001−14010

such as porphyrins.[14−17] However, each of these material classes has limitations. QACs are highly effective against enveloped viruses but are not effective against nonenveloped viruses[18,19] and typically would require regeneration when the compounds run out. Metals are effective against both enveloped and nonenveloped viruses, but they often involve the use of nanoparticles or salts to achieve optimal antiviral properties, thanks to the release of metal ions (typically Cu^{+}, Cu^{2+}, and Ag^{+}). These ions can be toxic and eventually will end up being released into the environment. Photosensitizers do not have toxicity concerns and are also highly effective but require complex synthesis and purification. The selection of materials should consider that antiviral surface coatings will potentially be used on a large scale; hence, sustainability and biocompatibility are two fundamental requisites. Ideal materials for antiviral surfaces should meet the following requirements: (1) high efficiency in viral inactivation, (2) environmental sustainability, (3) limited toxicity, and (4) low cost and scalability. Herein, we report the development and investigation of antiviral coatings purely made of lignin, a highly available plant-derived polymer, which satisfies these four conditions.[20−22] While a number of solution-based studies have demonstrated the ability of various lignin derivatives to inhibit viral entry in cells,[23−30] the use of lignin as an antiviral surface coating has not yet been explored.

Lignin is one of the main components of biomass, discarded in large amounts as a byproduct of the paper industry.[22,31] The complex aromatic structure of lignin provides this polymer with valuable properties such as antioxidant, UV-barrier, and antimicrobial activity;[21,32] hence, significant attention has been given to a wide-scale use of lignin-derived products in various applications.[20,31,33] In this study, five types of water-insoluble lignins were applied as a surface coating material that maintains efficient stability when incubated or washed with water. Two of the tested lignin types showed strong antiviral activity against Herpes Simplex Virus type 2 (HSV-2). The antiviral mechanism was attributed to the local generation of reactive oxygen species (ROS) upon exposure of the coatings to light. ROS include, for example, hydrogen peroxide (H_2O_2), superoxide anions (O_2^{-}), and hydroxyl radicals (HO·) that can be generated from molecular oxygen.[34] These reactive oxygen species can cause oxidative disruption of viruses by reacting with the amino acids present in their capsid and/or envelope.[14] ROS-mediated inactivation is considered to be an optimal mechanism for antiviral surfaces because it involves the release of nontoxic species that can be generated over a long time, removing the requirement for regeneration.[14] Lignin phenols can oxidize into quinones through a radical process,[35] inducing the reduction of molecular oxygen into ROS.[36] Thanks to their high efficiency in viral inactivation and their natural origin, the coatings described in this work represent a new development toward the achievement of affordable and environmentally sustainable antiviral and antimicrobial surfaces.

EXPERIMENTAL SECTION

Materials. All chemicals were used as received unless specified otherwise. Soda lignin (Protobind 1000) was purchased from Tanovis AG, Switzerland. Kraft lignin (UPM's BioPiva 100) was purchased from UPM Biochemicals, Finland. Organosolv lignin, terephthalic aldehyde-protected lignin (TALD lignin), and acid-catalyzed phenolated TALD lignin (TALD-APH lignin) were prepared in the Laboratory of Sustainable and Catalytic Processing of EPFL, as reported below. The lignins were dried in a vacuum oven at 45 °C for 24 h before being used. 2-Chloro-4,4,5,5-tetramethyl-1,3,2-dioxaphospholane (TMDP), cyclohexanol, deuterated chloroform, deuterated dimethylformamide, and anhydrous pyridine were provided by Sigma-Aldrich. Chromium(III) acetylacetonate and 1,4-dioxane were purchased from Acros Organics. Quantitative Peroxide Assay Kit was purchased from Thermo Fisher Scientific, Life Technologies. Phosphate buffered saline (PBS) tablets pH = 7.4 were purchased from AppliChem GmbH, Germany. Deionized water was obtained from a Millipore Direct-Q 5 ultrapure water system. Dulbecco's modified Eagle's Medium (DMEM) with GlutaMAX and Fetal bovine serum (FBS) were purchased from Life Technologies. 1% penicillin/streptomycin (P/S) was purchased from Thermo Fisher. Methyl cellulose and crystal violet were purchased from Sigma-Aldrich. Vero cells (African green monkey fibroblastoid kidney cells) and Madin-Darby canine kidney (MDCK) cells were purchased from ATCC. Vero E6 cells (Vero C1008, ATCC CRL-1586) were kindly provided by Prof. G. Kobinger (University of Texas). HSV-2 (herpes simplex virus type 2) was provided by M. Pistello (University of Pisa, Italy). Influenza virus A/Netherlands/602/2009 (H1N1)[37] was a kind gift from Prof. M. Schmolke (University of Geneva, Switzerland). SARS-CoV-2 (severe acute respiratory syndrome coronavirus) B.1.1.7 variant (hCoV-19/Switzerland/un-2012212272, EPI_ISL_2131446) was a generous gift from Prof. I. Eckerle (University Hospital of Geneva, Switzerland).

Methods. *Lignin Extraction and Modification.* Lignin extraction and acid phenolation were performed following the procedures previously published by Bertella et al.[38] In brief, for the organosolv lignin extraction, birch wood chips (*Betula pendula*) were stirred in an 80:20 ethanol/H_2O solution. HCl was added, and the solution was refluxed under vigorous stirring for 5 h. The solid residue was filtered, washed with ethanol, and dried under reduced pressure. The lignin was then dissolved in acetone, precipitated in deionized water, filtered, and dried. For further purification, the lignin was dissolved in dioxane and precipitated in diethyl ether. The precipitate was then filtered and dried overnight in a vacuum oven at 45 °C.

For the extraction TALD lignin, birch wood chips and terephthalic aldehyde were stirred in dioxane. Hydrochloric acid was added to the mixture, which was then heated at 85 °C for 3 h under vigorous stirring. The reaction mixture was then filtered. The filtrate was evaporated in a rotary evaporator, redissolved in fresh dioxane, precipitated in diethyl ether, and stirred for 1 h to dissolve most of the carbohydrates and unreacted terephthalic aldehyde. The mixture was then filtered and purified overnight with a Soxhlet extractor using diethyl ether as a solvent to remove all impurities. The washed solid was then dried overnight in a vacuum oven at 45 °C to obtain TALD lignin.

To prepare TALD-APH lignin, TALD lignin was stirred in molten phenol in the presence of concentrated H_2SO_4 for 30 min at 110 °C. The reaction was then cooled to room temperature, and DMSO was added to dilute the reaction. The resulting solution was added dropwise to deionized water previously adjusted to pH 1 with H_2SO_4. After the precipitation, the phenolated lignin was filtered and washed with water until the filtrate's pH was measured as neutral with pH indicator strips. The collected lignin was then dried overnight in a vacuum oven at 45 °C.

Lignin Characterization. To perform ^{31}P nuclear magnetic resonance spectroscopy (^{31}P NMR), the lignin hydroxyl groups were phosphorylated with 2-chloro-4,4,5,5-tetramethyl-1,3,2-dioxaphospholane (TMDP). Briefly, 20 mg of the sample was weighted and stirred overnight at room temperature in 400 μL of a 0.8: 0.8: 1 v/v mixture of deuterated $CHCl_3$, deuterated DMF, and anhydrous pyridine. Using the same solvent mixture, a solution containing 4 mg of chromium(III) acetylacetonate as a relaxation agent and 0.082 mmol of cyclohexanol as an internal standard was prepared and added to the lignin solution. Then, 100 μL of TMDP was added, and the mixture was transferred into an NMR tube previously fluxed with Argon and sealed with a septum. The phosphorylation reaction is completed within a few minutes, and the products are stable under an

https://doi.org/10.1021/acssuschemeng.2c04284
ACS Sustainable Chem. Eng. 2022, 10, 14001−14010

inert atmosphere. NMR spectra were recorded the same day on a Bruker AVANCE III 400 MHz spectrometer.

Gel permeation chromatography (GPC) analysis was performed on a SECcurity^2 GPC system (PSS Polymer Standards Service GmbH, Germany) equipped with a SECcurity^2 refractive index detector, a GRAM precolumn of 50 mm length, and three GRAM columns of 300 mm length. All columns have a diameter of 8 mm and a particle size of 20 μm. Sample analysis was performed in dimethylacetamide (DMAc) + 0.1 wt % LiBr at 70 °C at a flow rate of 1.0 mL/min, using poly(methyl methacrylate) (PMMA) standards.

Lignin Coating Preparation. To prepare the lignin coatings, 50 mg/mL lignin solutions in 1,4-dioxane were prepared by stirring at room temperature for 4 h. After that, the solutions were spin-coated on silicon wafers (2 cm × 2 cm size, 5 mm thickness). Before spin-coating, substrates were cleaned via sonication for 10 min in methanol, deionized water, and acetone and placed in a Femto Oxygen Plasma system (200 W, Diener Electronic) under 5 mL/min oxygen flow for 15 min. Then, 120 μL of the solution was deposited on the wafer, completely covering its surface, and then spin-coating was performed at 2000 rpm for 80 s using a Convac ST 146 spin coater. The samples were annealed at 120 °C for 30 min and dried under vacuum overnight at room temperature. The coatings were then incubated in water for 24 h to remove the possible unstable parts and finally dried again at room temperature before characterization.

Lignin Coating Characterization. For scanning electron microscopy (SEM) analysis, lignin coatings on silicon wafers were coated with a 7 nm protective layer of gold using a Q150T Plus, Quorum Technologies instrument. Images were captured using a Zeiss GeminiSEM 300 at 3.00 kV.

Atomic force microscopy (AFM) images were recorded using an Asylum Research Cypher VRS instrument (Oxford Instruments, United Kingdom). Measurements were done in tapping mode using a trihedral aluminum coated silicon cantilever (HQ/NSC14/Al BS, MikroMasch, Hungary) with 5 N/m spring constant and ∼160 kHz resonance frequency. The roughness average (R_a) was calculated using Gwyddion software.

Water contact angle measurements were performed using a DataPhysics OCA 35 contact angle measurement instrument in ambient conditions. A 15 μL Milli-Q water droplet was used for each measurement. The contact angle was determined using software SCA 20 from DataPhysics. The reported values are given as the average value of at least 3 measurements ± standard deviation.

Antiviral Activity Test by Plaque Assay. Herpes Simplex Virus Type 2 (HSV-2). The antiviral activity of the lignin surfaces against the Herpes Simplex Virus type 2 (HSV-2) strain was titrated by plaque assay on Vero cells (African green monkey fibroblastoid kidney cells). Cells were cultured in Dulbecco's modified Eagle's medium (DMEM-GlutaMAX, Gibco/BRL, Gaithersburg, MD) supplemented with 10% heat-deactivated fetal bovine serum (FBS, Gibco/BRL, Gaithersburg, MD) and 1% penicillin/streptomycin (P/S, Gibco/BRL, Gaithersburg, MD). The cell line was grown in 5% CO_2 humidified atmosphere at 37 °C. Vero cells were plated in 96-well plates for 24 h before performing the antiviral test, considering a density of 1.45 × 10^4 cells/well. After checking for full cell confluency on the day of the experiment, the cell medium was changed to DMEM/2%FBS/1% P/S just before running the plaque assay.

The antiviral activity of the surfaces was tested following wet-to-dry and wet-to-wet protocols. The two protocols differ in the way in which the virus sample is collected from the surface at the end of the inoculation time. All data presented in each plot correspond to one single experiment to avoid variations of environmental conditions. Each experiment was repeated multiple times. Surfaces were placed inside airtight Petri dishes, and 80 μL of virus inoculum (∼10^5 pfu/mL) was carefully spread all over the surface to be tested. For the wet-to-dry test, the virus inoculum was allowed to dry for 30 min without closing the Petri dish. The residual virus on the surface was collected with a sterile swab prewetted with 30 μL DMEM-GlutaMAX/2% FBS/1%P/S. The swab was inserted into a vial containing 970 μL DMEM-GlutaMAX/2%FBS/1%P/S and vortexed for 1 min. For time course experiments, multiple time points were added (45, 60, and 75 min) for the sample collection. For the wet-to-wet test, after spreading the virus inoculum, the airtight Petri dish was closed to prevent evaporation. After 30 min, the Petri dish was opened, and the surface was thoroughly rinsed with 1000 μL DMEM-GlutaMAX/2%FBS/1% P/S to recover the virus. For time course experiments, multiple time points were added (60, 90, and 120 min) for the sample collection.

For both protocols, Vero cells were infected with the collected sample by transferring it to the first row of the 96-well plate and performing serial 10× dilutions. The cell infection was allowed to proceed for 1 h at 37 °C, and then the cell medium was discarded. The cells were overlaid with medium containing 1.2% methyl cellulose and incubated overnight at 37 °C. On the day after, cells were fixed and stained with 0.1% of crystal violet in 20% ethanol. Plaques were counted in each well to determine the recovered infective virus from each surface.

Influenza Virus. The antiviral activity of the lignin surfaces against Influenza virus was titrated by plaque assay on MDCK cells. Cells were cultured in DMEM-GlutaMAX medium supplemented with 10% FBS and 1% P/S. MDCK cells were plated in 6-well plates for 24 h before performing the antiviral test, considering a density of 8.5 × 10^5 cells/well. After checking for full cell confluency on the day of the experiment, the cells were washed with PBS +/+ (with $MgCl_2$ and $CaCl_2$), and the medium was changed to DMEM/1%P/S just before running the plaque assay. The wet-to-dry protocol was followed to evaluate the surface antiviral activity. 10-fold serial dilutions of the recovered viral inoculum were prepared in DMEM-GlutaMAX/1%P/S to infect the cells at 37 °C with 5% CO_2 for 1 h. Then, the cell medium was discarded, and the cells were overlaid. The overlay solution was prepared from a 2× MEM stock supplemented with 4 mM L-glutamine, 0.24% $NaHCO_3$, 0.02 M HEPES, 0.2 mg/mL P/S, and 0.42% BSA. The 2× MEM stock solution was diluted 1:1 and supplemented with 0.6% agar, 1 μg/mL TPCK trypsin, 0.1 μg/mL DEAE dextran, and 1 mg/mL $NaHCO_3$. After 48 h of incubation at 37 °C, the cells were fixed with 4% paraformaldehyde solution and stained with 0.5% crystal violet. Plaques were counted in each well to determine the recovered infective virus from each surface.

SARS-CoV-2. The antiviral activity of the lignin surfaces against SARS-CoV-2 was tested by performing a plaque assay on the virus collected according to the wet-to-try protocol described above. The experiment was performed under biosafety level 3 (BSL-3) environment. Vero E6 cells were plated in 24-well plates 24 h before the plaque assay (10^5 cells/well) to reach confluency. 3-fold serial dilutions of the recovered viral inoculum were prepared in DMEM-GlutaMAX/2.5%FBS/1%P/S to infect the cells at 37 °C with 5% CO_2. Then, following the removal of viral inoculum, cells were overlaid with DMEM-GlutaMAX/2.5%FBS/1%P/S containing 0.4% Avicel GP3515 and incubated at 37 °C with 5% CO_2 for 48 h. The overlay medium was then removed, and cells were fixed with 4% PFA and stained with 0.1% crystal violet in 20% ethanol. Plaques were counted in each well to determine the recovered infective virus from each surface. Each surface was analyzed in duplicate.

H_2O_2 Quantification via Ferrous Oxidation−Xylenol Orange (FOX) Assay. Lignin coatings prepared on fused silica substrates (0.8 cm × 0.8 cm size, 5 mm thickness) were placed at the bottom of 4 mL plastic cuvettes (1 cm × 1 cm base size), and 0.4 mL PBS (pH = 7.4) was added to each of them. One cuvette was irradiated from the top for 1, 2, 3, and 4 h with visible light at an intensity of 50 mW/cm^2 (Schott KL 1600 LED lamp), while a second one was kept in the dark as control. After each time point, 50 μL was transferred in an Eppendorf, and the H_2O_2 concentration was quantified using the Quantitative Peroxide Assay Kit by following the procedure provided by the supplier. Then, 5 μL of reagent A (25 mM ammonium ferrous(II) sulfate, 2.5 M H_2SO_4) and 500 μL of reagent B (100 mM sorbitol, 125 μM xylenol orange in water) were added to each Eppendorf and left for 1 h in the dark. The mixture was transferred to a cuvette, and the absorbance was recorded between 500 and 700 nm using a PerkinElmer Lambda 365 UV−visible spectrophotometer. Clean fused silica substrates were also tested as controls. The experiment was performed in triplicate, and the results were reported

https://doi.org/10.1021/acssuschemeng.2c04284
ACS Sustainable Chem. Eng. 2022, 10, 14001−14010

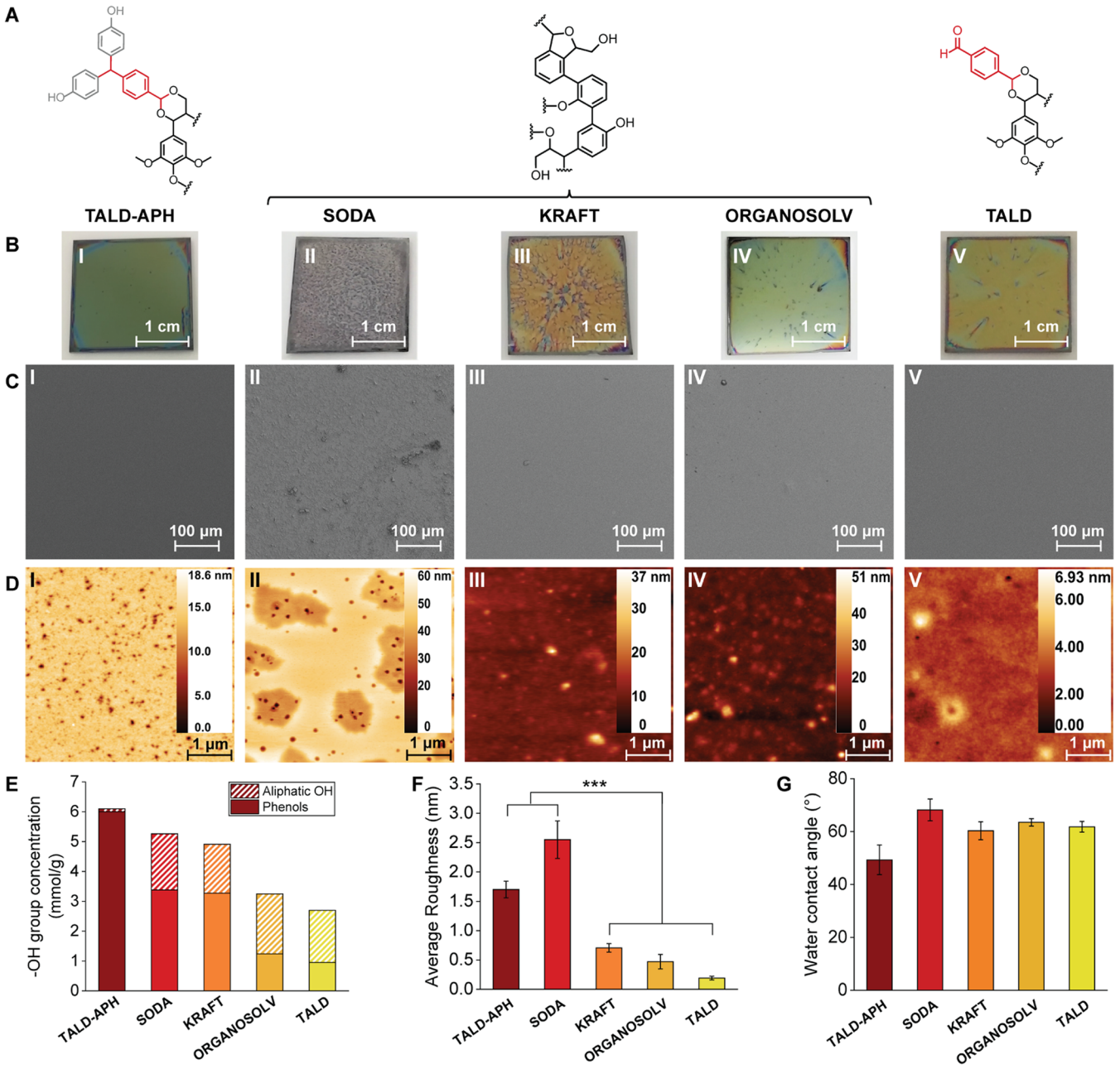

Figure 1. (A) Schematic representation of a structural unit of the various lignins used in this study. Representative (B) optical micrographs, (C) SEM images, and (D) AFM images of coatings made of (I) TALD-APH, (II) Soda, (III) Kraft, (IV) Organosolv, and (V) TALD. (E) Plot of the hydroxyl group concentration per gram of lignin quantified by ^{31}P NMR spectroscopy. (F) Plot of the average roughness (R_a) of the lignin coatings measured by AFM. (G) Plot of water contact angle of the lignin coatings. Statistical analysis was performed with a one-way analysis variance (ANOVA) with a Tukey comparison post hoc test (***: $p < 0.001$).

as mean ± standard deviation. A calibration curve was prepared by testing a series of solutions containing 0−30 μM H_2O_2.

RESULTS AND DISCUSSION

Lignin Coating Preparation and Characterization. Lignin can be obtained from biomass via several different extraction processes, the Sulfite, Soda, Kraft, Organosolv, and the aldehyde-assisted fractionation (AAF) process.[39−41] Each process generates lignin with different molecular weights, chemical compositions, and types of impurities.[20,41,42] While the Sulfite process generates lignosulfonates,[41] which are water-soluble salts, the lignins obtained with the other methods are insoluble in water at neutral pH[41] and can thus be used as surface coating materials. Consequently, Soda, Kraft, and Organosolv lignin were investigated together with two chemically modified lignins that were obtained via the AAF process, viz. terephthalic aldehyde-protected lignin (TALD) and phenolated terephthalic aldehyde lignin (TALD-APH). These last two lignins are known to present very low and very high phenol content, respectively.[38] A representative structural unit of these five lignins is shown in Figure 1A, while a more complete scheme of the structure is provided in Scheme S1. All lignins were analyzed by GPC to determine their molecular weight (Table S1), and by ^{31}P NMR spectroscopy to determine the hydroxyl group content (see spectra in Figure S1 and calculated concentration of −OH groups of different

https://doi.org/10.1021/acssuschemeng.2c04284
ACS Sustainable Chem. Eng. 2022, 10, 14001−14010

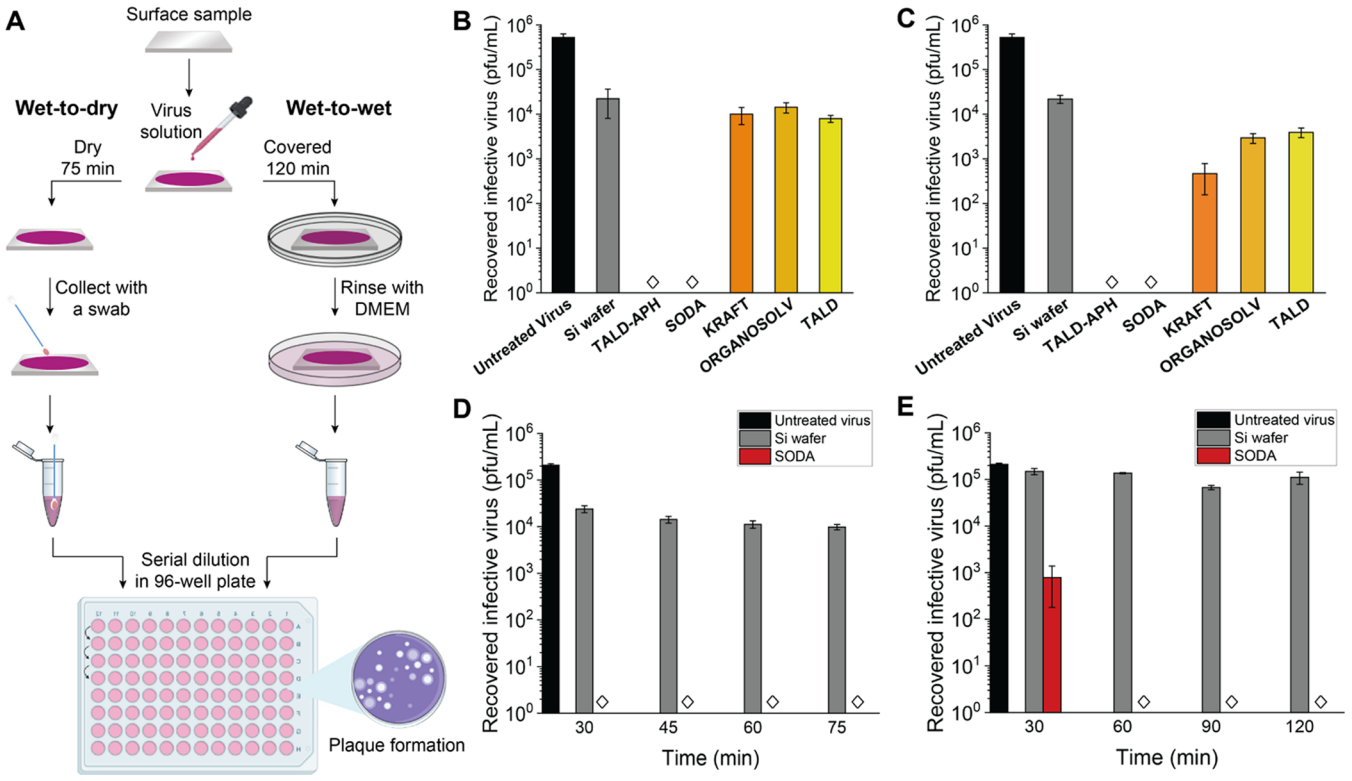

Figure 2. (A) Illustration of the wet-to-dry and wet-to-wet protocols used to assess surface virucidal activity. Created with Biorender (biorender.com). (B) Antiviral activities of lignin surfaces tested according to the wet-to-dry protocol. (C) Antiviral activities of lignin surfaces tested according to the wet-to-wet protocol. (D, E) Time course of virucidal activity: HSV-2 was exposed to Soda lignin coatings for different time periods and then serially diluted on Vero cells; (D) antiviral activities tested according to the wet-to-dry protocol; and (E) antiviral activities tested according to the wet-to-wet procedure. Clean silicon wafers were also tested in the same conditions as control. ◊ = below detection limit of 125 PFU/mL. "Untreated virus" stands for the original viral stock used for the test.

natures in Table S2). As a result of the different processes that were used for their isolation, gel permeation chromatography (GPC) analyses revealed large differences in molecular weight and dispersity across the different lignins (M_n = 900−2300 g/mol, M_w = 1500−12,000 g/mol, and $Đ$ = 1.5−6.7, Table S1). Figure 1E presents the hydroxyl group content of the different lignins, as determined by ^{31}P NMR spectroscopy. TALD-APH and Soda lignin present the highest concentration of phenols among the five lignins that we find plays a central role in ROS generation on the lignin surface, as will be explained below.

Coatings from these different lignins were prepared by spin-coating 50 mg/mL dioxane solutions on clean and plasma-treated silicon wafers. Optical micrographs of the surfaces are shown in Figure 1B, and higher magnification images are presented in Figure S2. Scanning electron microscopy (SEM) and atomic force microscopy (AFM) images (Figures 1C,D, respectively) show that spin coating generates uniform coatings with a thickness of ∼200 nm (see Figure S3 for thickness determination, and Figure S4 for SEM images at higher magnification). In Figure 1F, the average roughness (R_a) of the coatings is compared, indicating that TALD-APH and Soda lignin present significantly larger roughnesses compared to the other three lignin types. To study the effect of the polymer concentration used during spin coating on the structure and properties of the lignin coatings, Kraft lignin films were also prepared from solutions with polymer concentrations of 100 and 200 mg/mL. This afforded films with thicknesses of 0.6 and 1.6 μm, as compared to 0.18 μm when coatings were prepared using a 50 mg/mL solution. AFM analysis did not reveal any significant effects of the polymer concentration on the structure and surface roughness of the films (see Figure S5). Figures 1G and S6 present the results of the water contact angle analyses that were performed on all 5 lignin coatings. All of the coatings showed similar values with no statistically significant difference. The results presented in Figure 1 were obtained on spin-cast films that were incubated in water for a period of 24 h prior to analysis and thus also illustrate the stability of these coatings.

Antiviral Activity. As a virus to assess the antiviral activity of the coatings, we chose HSV-2. The antiviral activity of the lignin coating against HSV-2 was evaluated using two different protocols (that we call wet-to-dry and wet-to-wet) adapted from the literature (Figure 2A).[43−45] These two protocols emulate two real-life situations. The wet-to-dry protocol emulates the most common real-life scenario in which the viral inoculum evaporates on the tested surface, whereas the wet-to-wet protocol does not allow for evaporation of the viral inoculum. To assess the antiviral activity of lignin coatings, the infectivity of HSV-2 was measured by the plaque assay after recovering the viral inoculum either after 75 min (wet-to-dry) or 120 min (wet-to-wet). The incubation times were chosen according to the previously published protocols.[43,44] Results are shown in Figure 2B (wet-to-dry) and Figure 2C (wet-to-wet). TALD-APH and Soda lignin showed a decrease in viral titer below the limit of detection (>99% inactivation); all other types of lignin basically showed an activity comparable to the silicon wafer control. Analysis of Kraft lignin films of different film thicknesses, which were obtained by spin-coating solutions

https://doi.org/10.1021/acssuschemeng.2c04284
ACS Sustainable Chem. Eng. 2022, 10, 14001−14010

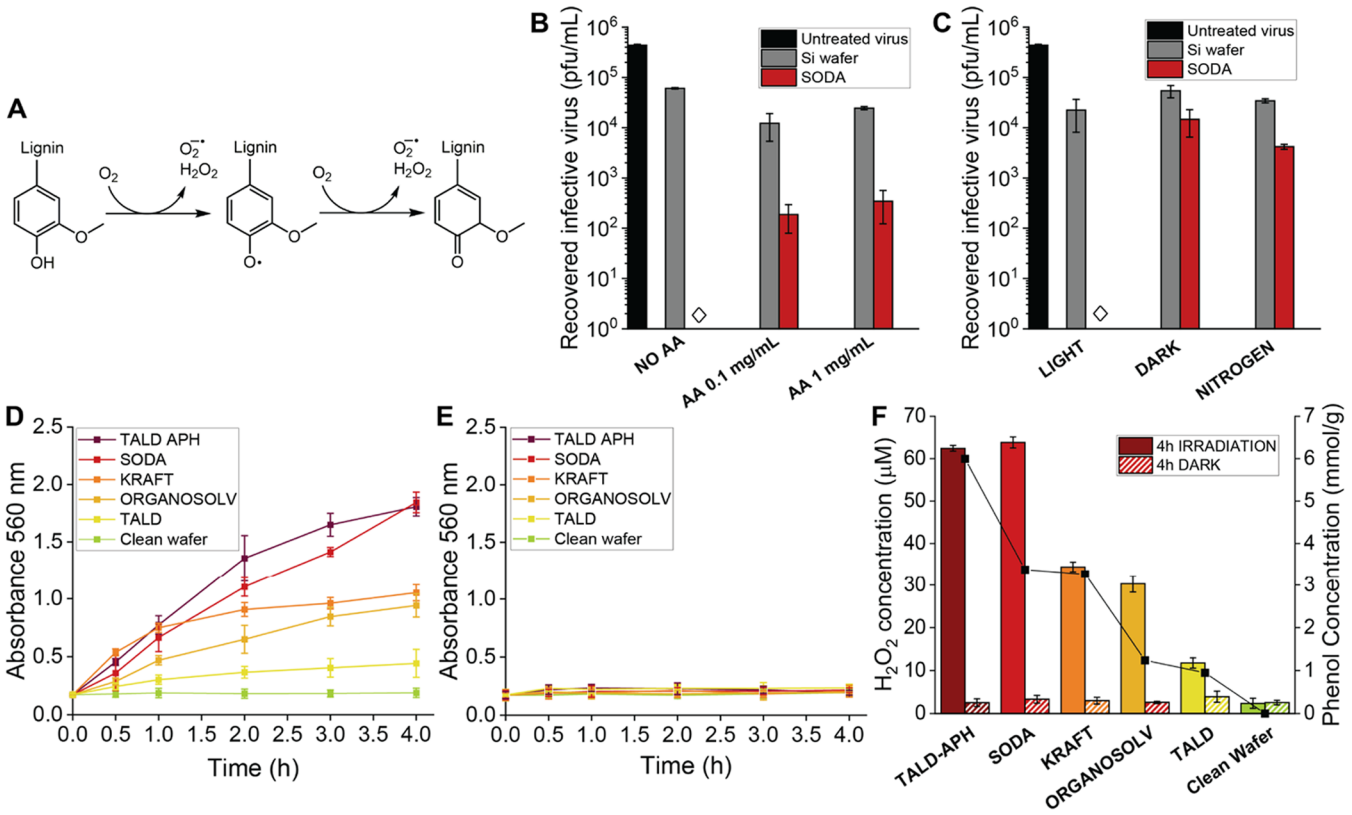

Figure 3. (A) Proposed ROS generation process: upon irradiation with visible light, lignin undergoes oxidation, which generates ROS as intermediates. (B) Wet-to-dry virucidal tests for soda lignin surfaces in the presence of L-ascorbic acid (AA). (C) Wet-to-dry virucidal tests for Soda lignin surfaces performed in the light, in the dark, and under N_2. Clean silicon wafers were also tested in the same conditions as control. ◊ = below detection limit of 125 PFU/mL. "Untreated virus" stands for the original viral stock used for the test. (D, E) Time-dependent H_2O_2 generation from the lignin coatings detected by the FOX assay: (D) coatings irradiated with visible light with intensity 50 mW/cm^2, (E) coatings kept in the dark. The data are reported as the average of at least three measures, and the error bars represent the standard deviation. (F) Concentration of the H_2O_2 generated from the different lignin coatings after 4 h of irradiation or in the dark, calculated using the calibration curve reported in Figure S5C (*y*-axes on the left), correlated with the lignin phenol concentration (*y*-axes on the right).

with different polymer concentrations, did not reveal any influence of film thickness on the antiviral activity (Figure S7). To understand how incubation time affects antiviral activity, we performed antiviral time course studies on Soda lignin substrates according to both wet-to-dry and wet-to-wet protocols. The viral inoculum was recovered at four time points (t = 30, 45, 60, 75 min for wet-to-dry and t = 30, 60, 90, 120 min for wet-to-wet) from the start of viral incubation (t = 0). Results are shown in Figure 2D (wet-to-dry) and Figure 2E (wet-to-wet). The wet-to-dry time course showed a major drop of the viral titer during the drying process (i.e., the period between the time point at which the viral inoculum dried on the surface and the time point at which the sample was collected) as the virus was already fully inactivated at t = 30 min (i.e., the viral inoculum was just dried). The wet-to-wet time course showed that under wet conditions, the total virus inactivation takes longer (between 30 and 60 min) than under the wet-to-dry scenario. This observation may be attributed to the lower stability of viruses upon drying.[46]

ROS Generation from the Lignin Coatings. Oxidation of lignin phenols into quinones via radical intermediates can induce the reduction of molecular oxygen and the formation of ROS that in turn could contribute to the observed antiviral activity of the surface coatings (a scheme of the proposed mechanism is reported in Figure 3A).[35,36,41] To verify the possible involvement of ROS in the inactivation process, the wet-to-dry antiviral test was performed in the presence of ascorbic acid (AA), a reducing agent known to scavenge free radicals and ROS in physiological conditions.[47,48] AA at two different concentrations (1 and 0.1 mg/mL) was dissolved into HSV-2 viral stock prior to inoculation, and 75 min wet-to-dry incubation was done on Soda lignin coatings and Si wafers (as control). The outcome of the test, reported in Figure 3B, indicates that the antiviral activity of the Soda lignin coatings is reduced in the presence of AA. This result is consistent with our hypothesis that ROS are involved in the antiviral mechanism.

To further corroborate the presumed mechanism, the wet-to-dry antiviral activity test was performed either in the dark or in the absence of O_2, two conditions known to decrease the generation of ROS from the coatings.[36,49] The results in Figure 3C present a drastic reduction in the antiviral activity of the coatings under these two conditions, which illustrates the role of ROS.

As a model ROS compound, H_2O_2 generated from the lignin coatings was quantified by the ferrous oxidation−xylenol orange (FOX) assay. In Figure S8, we illustrate the FOX assay mechanism and show a calibration curve obtained measuring H_2O_2 solutions at different concentrations. To measure the H_2O_2 generated by the coatings in conditions analogous to the antiviral tests, coated substrates were immersed in PBS at pH = 7.4 and irradiated with visible light. As control, the test was

https://doi.org/10.1021/acssuschemeng.2c04284
ACS Sustainable Chem. Eng. 2022, 10, 14001−14010

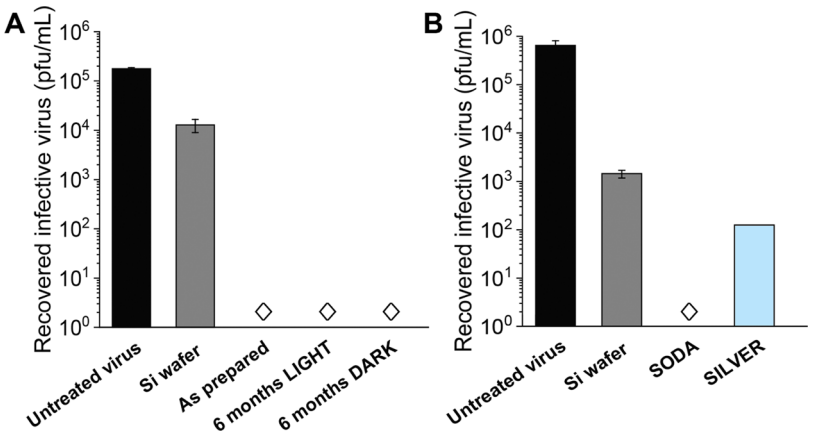

Figure 4. (A) Wet-to-dry virucidal tests for soda lignin surfaces freshly prepared and stored for 6 months in ambient conditions in the dark or under the sunlight. (B) Wet-to-dry virucidal tests for Soda lignin surfaces and silver-coated surfaces. Clean silicon wafers were also tested in the same conditions as control. ◊ = below detection limit of 125 PFU/mL. "Untreated virus" stands for the original viral stock used for the test.

also performed in the dark, and uncoated substrates were tested as well. The absorbance spectra obtained during the test are reported in Figure S9, and the outcome of the tests is summarized in Figure 3D (test performed under light irradiation) and Figure 3E (test performed in the dark). From the values of maximum absorbance (560 nm), using the calibration curve, the corresponding H_2O_2 concentrations were calculated and plotted in Figure 3F. After 4 h of light irradiation, Soda and TALD-APH lignin surfaces produced 2−6 times more H_2O_2 compared to the other three species of lignin. This observation is consistent with the stronger antiviral activity observed for these two coating types. We should also point out that in the dark, a low concentration of H_2O_2 was detected at each time point, in agreement with the poor antiviral activity measured during the wet-to-dry test performed in the absence of light.

Regarding the calculated H_2O_2 concentration (2−64 μM, depending on the lignin type), it is important to underline that these values are relative to the experimental setup used to perform the FOX assay on the surface, which means in different conditions compared with the ones virus is experiencing during the antiviral test. In any event, in realistic conditions, a mixture of many ROS species is generated at the solid−liquid interface, where high local concentrations of these species exist. Hence, the FOX assay gives only an indication of the proposed mechanism.

It is interesting to compare the results in Figure 3F with those presented in Figures 2B,C, and 1E. While Figure 1E does not show a large difference in the total hydroxyl group content between TALD-APH, Soda, and Kraft lignin, Figure 2B,C reveals large differences in antiviral activity between TALD-APH and Soda lignin on the one hand, and Kraft lignin on the other hand. The differences between these two sets of results reflect the fact that the hydroxyl group contents that are presented in Figure 1E were determined in solution, while the antiviral activities and H_2O_2 generation that are shown in Figures 2 and 3 were determined on solid polymer coatings.

The virucidal activity of the lignin coatings was further studied toward two additional viruses: Influenza A and SARS-CoV-2. The results of these experiments are shown in Figure S10 and indicate that the lignin coatings do not show a significant antiviral activity against these two viruses. As SARS-CoV-2 is relatively insensitive toward H_2O_2,[50−55] these results support the role of ROS in the antiviral activity of the lignin coatings toward HSV-2.

Lignin Coating Aging and Comparison with Benchmark. The durability of the Soda lignin coatings was tested over a period of 6 months. During this time, the coated surfaces were stored in ambient conditions in the dark or in the laboratory close to a window so as to be exposed to sunlight. As shown in Figure 4A, the coatings that were stored in both conditions maintained their antiviral activity and showed complete inactivation of HSV-2, as observed for the freshly prepared samples. In a final experiment, the performance of the Soda lignin-based coating was compared against a silver-coated surface, which is a well-known antiviral material,[14,15] as a benchmark. Considering the test detection limit of 125 PFU/mL, from the results reported in Figure 4B, the antiviral activity of Soda lignin and silver was comparable.

CONCLUSIONS

This study has investigated the use of lignin, a plant-derived polymer, for application as an antiviral coating. From the five different types of lignin that were tested (TALD-APH, Soda, Kraft, Organosolv, and TALD), TALD-APH and Soda lignin showed strong antiviral activity against herpes simplex virus type 2 (HSV-2). The antiviral activity of these two lignins was attributed to the local generation of reactive oxygen species that results from the oxidation of phenolic hydroxyl groups in lignin. The Soda lignin coatings had antiviral activities toward HSV-2 that are comparable with those of silver, a well-known antiviral material, and retained their antiviral activity for at least 6 months of storage in ambient conditions. This study shows that lignin is a promising material for the development of efficient and sustainable antimicrobial coatings.

ASSOCIATED CONTENT

Supporting Information

The Supporting Information is available free of charge at https://pubs.acs.org/doi/10.1021/acssuschemeng.2c04284.

Schematic illustration of the chemical structure and characterization of the utilized lignin; molecular weights determined by GPC; hydroxyl group concentrations of lignin obtained from ^{31}P NMR spectroscopy; ^{31}P NMR spectra; high-magnification optical microscopy images; AFM images; high-magnification SEM images; water

https://doi.org/10.1021/acssuschemeng.2c04284
ACS Sustainable Chem. Eng. 2022, 10, 14001−14010

contact angles; antiviral activities of Kraft lignin surfaces with different film thicknesses tested according to wet-to-dry protocol against HSV-2; mechanism and calibration of FOX assay; typical absorbance spectra of FOX assay performed on sample surfaces, and antiviral activities of soda lignin surfaces tested according to wet-to-dry protocol against Influenza A and SARS-CoV-2 (PDF)

AUTHOR INFORMATION

Corresponding Authors

Harm-Anton Klok − *Institut des Matériaux and Institut des Sciences et Ingénierie Chimiques, Laboratoire des Polymères, École Polytechnique Fédérale de Lausanne (EPFL), CH-1015 Lausanne, Switzerland;* orcid.org/0000-0003-3365-6543; Email: harm-anton.klok@epfl.ch

Francesco Stellacci − *Institute of Materials and Institute of Materials, Department of Bioengineering and Global Health Institute, École Polytechnique Fédérale de Lausanne (EPFL), CH-1015 Lausanne, Switzerland;* orcid.org/0000-0003-4635-6080; Email: francesco.stellacci@epfl.ch

Authors

Alice Boarino − *Institut des Matériaux and Institut des Sciences et Ingénierie Chimiques, Laboratoire des Polymères, École Polytechnique Fédérale de Lausanne (EPFL), CH-1015 Lausanne, Switzerland*

Heyun Wang − *Institute of Materials, École Polytechnique Fédérale de Lausanne (EPFL), CH-1015 Lausanne, Switzerland;* orcid.org/0000-0001-6764-4220

Francesca Olgiati − *Institute of Materials, École Polytechnique Fédérale de Lausanne (EPFL), CH-1015 Lausanne, Switzerland*

Fiora Artusio − *Institute of Materials, École Polytechnique Fédérale de Lausanne (EPFL), CH-1015 Lausanne, Switzerland;* orcid.org/0000-0002-8996-0053

Melis Özkan − *Institute of Materials, École Polytechnique Fédérale de Lausanne (EPFL), CH-1015 Lausanne, Switzerland*

Stefania Bertella − *Laboratory of Sustainable and Catalytic Processing, Institute of Chemical Sciences and Engineering, École Polytechnique Fédérale de Lausanne (EPFL), CH-1015 Lausanne, Switzerland;* orcid.org/0000-0002-1381-6274

Nicolò Razza − *Institute of Materials, École Polytechnique Fédérale de Lausanne (EPFL), CH-1015 Lausanne, Switzerland;* orcid.org/0000-0002-6635-8254

Valeria Cagno − *Institute of Microbiology, Lausanne University Hospital, University of Lausanne, CH-1011 Lausanne, Switzerland*

Jeremy S. Luterbacher − *Laboratory of Sustainable and Catalytic Processing, Institute of Chemical Sciences and Engineering, École Polytechnique Fédérale de Lausanne (EPFL), CH-1015 Lausanne, Switzerland;* orcid.org/0000-0002-0967-0583

Complete contact information is available at: https://pubs.acs.org/10.1021/acssuschemeng.2c04284

Author Contributions

#A.B. and H.W. contributed equally to this work.

Notes

The authors declare the following competing financial interest(s): S.B. and J.S.L. are inventors on a European patent application (EP19202957) that was submitted by EPFL and covers the isolation of different functionalized lignins via the aldehyde assisted fractionation process. J.S.L. is co-founder and part owner of Bloom Biorenewables Ltd that aims at commercializing the aldehyde assisted fractionation process.
S.B. and J.S.L. are inventors on a European patent application (EP19202957) that was submitted by EPFL and covers the isolation of different functionalized lignins via the aldehyde-assisted fractionation process. J.S.L. is the cofounder and part owner of Bloom Biorenewables Ltd that aims at commercializing the aldehyde-assisted fractionation process.

ACKNOWLEDGMENTS

A.B., S.B., J.S.L., and H.-A.K. acknowledge Swiss National Science Foundation (SNSF) Grant CRSII5_180258 for financial support. H.W. and F.S. acknowledge SNSF NCCR Bio-Inspired Materials funding and SNSF Grant 200020_185062 for financial support. M.Ö. acknowledges EU H2020 Project NeuTouch under Grant Agreement No. 813713 for financial support. The authors acknowledge Prof. I. Eckerle, Dr. M. Essaidi-Laziosi, and Dr. M. Bekliz (University Hospital of Geneva, Switzerland) for providing SARS-CoV-2 strains, Dr. M. Gasbarri (EPFL) for valuable discussions, and V. Padrun (EPFL) for supporting BSL-3 experiments.

REFERENCES

(1) Jayaweera, M.; Perera, H.; Gunawardana, B.; Manatunge, J. Transmission of COVID-19 Virus by Droplets and Aerosols: A Critical Review on the Unresolved Dichotomy. *Environ. Sci.* **2020**, *188*, No. 109819.

(2) Kitajima, M.; Ahmed, W.; Bibby, K.; Carducci, A.; Gerba, C. P.; Hamilton, K. A.; Haramoto, E.; Rose, J. B. SARS-CoV-2 in Wastewater: State of the Knowledge and Research Needs. *Sci. Total Environ.* **2020**, *739*, No. 139076.

(3) Aboubakr, H. A.; Sharafeldin, T. A.; Goyal, S. M. Stability of SARS-CoV-2 and Other Coronaviruses in the Environment and on Common Touch Surfaces and the Influence of Climatic Conditions: A Review. *Transbound Emerg Dis* **2021**, *68*, 296−312.

(4) Reina, G.; Iglesias, D.; Samorì, P.; Bianco, A. Graphene: A Disruptive Opportunity for COVID-19 and Future Pandemics? *Adv. Mater.* **2021**, *33*, No. 2007847.

(5) Wang, C. C.; Prather, K. A.; Sznitman, J.; Jimenez, J. L.; Lakdawala, S. S.; Tufekci, Z.; Marr, L. C. Airborne Transmission of Respiratory Viruses. *Science* **2021**, *373*, No. eabd9149.

(6) Gall, A. M.; Mariñas, B. J.; Lu, Y.; Shisler, J. L. Waterborne Viruses: A Barrier to Safe Drinking Water. *PLoS Pathog.* **2015**, *11*, No. e1004867.

(7) Xiao, S.; Tang, J.; Li, Y. Airborne or Fomite Transmission for Norovirus? A Case Study Revisited. *Int. J. Environ. Res. Public Health* **2017**, *14*, No. 1571.

(8) Boone, S. A.; Gerba, C. P. Significance of Fomites in the Spread of Respiratory and Enteric Viral Disease. *Appl. Environ. Microbiol.* **2007**, *73*, 1687−1696.

(9) Kraay, A. N. M.; Hayashi, M. A. L.; Hernandez-Ceron, N.; Spicknall, I. H.; Eisenberg, M. C.; Meza, R.; Eisenberg, J. N. S. Fomite-Mediated Transmission as a Sufficient Pathway: A Comparative Analysis across Three Viral Pathogens. *BMC Infect. Dis.* **2018**, *18*, No. 540.

(10) Wißmann, J. E.; Kirchhoff, L.; Brüggemann, Y.; Todt, D.; Steinmann, J.; Steinmann, E. Persistence of Pathogens on Inanimate Surfaces: A Narrative Review. *Microorganisms* **2021**, *9*, No. 343.

(11) Kambhampati, A.; Koopmans, M.; Lopman, B. A. Burden of Norovirus in Healthcare Facilities and Strategies for Outbreak Control. *J. Hosp. Infect.* **2015**, *89*, 296−301.

(12) Lin, Q.; Lim, J. Y. C.; Xue, K.; Yew, P. Y. M.; Owh, C.; Chee, P. L.; Loh, X. J. Sanitizing Agents for Virus Inactivation and Disinfection. *View* **2020**, *1*, No. e16.
(13) Costa, L.; Faustino, M. A. F.; Neves, M. G. P. M. S.; Cunha, Â.; Almeida, A. Photodynamic Inactivation of Mammalian Viruses and Bacteriophages. *Viruses* **2012**, *4*, 1034−1074.
(14) Wang, N.; Ferhan, A. R.; Yoon, B. K.; Jackman, J. A.; Cho, N.-J.; Majima, T. Chemical Design Principles of Next-Generation Antiviral Surface Coatings. *Chem. Soc. Rev.* **2021**, *50*, 9741−9765.
(15) Rakowska, P. D.; Tiddia, M.; Faruqui, N.; Bankier, C.; Pei, Y.; Pollard, A. J.; Zhang, J.; Gilmore, I. S. Antiviral Surfaces and Coatings and Their Mechanisms of Action. *Commun. Mater.* **2021**, *2*, No. 53.
(16) Kwon, K. Y.; Cheeseman, S.; Frias-De-Diego, A.; Hong, H.; Yang, J.; Jung, W.; Yin, H.; Murdoch, B. J.; Scholle, F.; Crook, N.; Crisci, E.; Dickey, M. D.; Truong, V. K.; Kim, T. A Liquid Metal Mediated Metallic Coating for Antimicrobial and Antiviral Fabrics. *Adv. Mater.* **2021**, *33*, No. 2104298.
(17) Liu, Q.; Zhang, Y.; Liu, W.; Wang, L.-H.; Choi, Y. W.; Fulton, M.; Fuchs, S.; Shariati, K.; Qiao, M.; Bernat, V.; Ma, M. A Broad-Spectrum Antimicrobial and Antiviral Membrane Inactivates SARS-CoV-2 in Minutes. *Adv. Funct. Mater.* **2021**, *31*, No. 2103477.
(18) Tuladhar, E.; de Koning, M. C.; Fundeanu, I.; Beumer, R.; Duizer, E. Different Virucidal Activities of Hyperbranched Quaternary Ammonium Coatings on Poliovirus and Influenza Virus. *Appl. Environ. Microbiol.* **2012**, *78*, 2456−2458.
(19) Fulmer, P. A.; Wynne, J. H. Development of Broad-Spectrum Antimicrobial Latex Paint Surfaces Employing Active Amphiphilic Compounds. *ACS Appl. Mater. Interfaces* **2011**, *3*, 2878−2884.
(20) Bajwa, D. S.; Pourhashem, G.; Ullah, A. H.; Bajwa, S. G. A Concise Review of Current Lignin Production, Applications, Products and Their Environmental Impact. *Ind. Crops Prod.* **2019**, *139*, No. 111526.
(21) Shu, F.; Jiang, B.; Yuan, Y.; Li, M.; Wu, W.; Jin, Y.; Xiao, H. Biological Activities and Emerging Roles of Lignin and Lignin-Based Products—A Review. *Biomacromolecules* **2021**, *22*, 4905−4918.
(22) Stewart, D. Lignin as a Base Material for Materials Applications: Chemistry, Application and Economics. *Ind. Crops Prod.* **2008**, *27*, 202−207.
(23) Kimura, C.; Li, R.; Ouda, R.; Nishimura, H.; Fujita, T.; Watanabe, T. Production of Antiviral Substance from Sugarcane Bagasse by Chemical Alteration of Its Native Lignin Structure through Microwave Solvolysis. *ChemSusChem* **2020**, *13*, 4519−4527.
(24) Li, R.; Ouda, R.; Kimura, C.; Narita, R.; Nishimura, H.; Fujita, T.; Watanabe, T. Conversion of Beech Wood into Antiviral Lignin−Carbohydrate Complexes by Microwave Acidolysis. *ACS Sustainable Chem. Eng.* **2021**, *9*, 9248−9256.
(25) Oeyen, M.; Noppen, S.; Vanhulle, E.; Claes, S.; Myrvold, B. O.; Vermeire, K.; Schols, D. A Unique Class of Lignin Derivatives Displays Broad Anti-HIV Activity by Interacting with the Viral Envelope. *Virus Res.* **2019**, *274*, No. 197760.
(26) Raghuraman, A.; Tiwari, V.; Zhao, Q.; Shukla, D.; Debnath, A. K.; Desai, U. R. Viral Inhibition Studies on Sulfated Lignin, a Chemically Modified Biopolymer and a Potential Mimic of Heparan Sulfate. *Biomacromolecules* **2007**, *8*, 1759−1763.
(27) Thakkar, J. N.; Tiwari, V.; Desai, U. R. Nonsulfated, Cinnamic Acid-Based Lignins Are Potent Antagonists of HSV-1 Entry into Cells. *Biomacromolecules* **2010**, *11*, 1412−1416.
(28) Vinardell, M.; Mitjans, M. Lignins and Their Derivatives with Beneficial Effects on Human Health. *Int. J. Mol. Sci.* **2017**, *18*, No. 1219.
(29) Lee, J.-B.; Yamagishi, C.; Hayashi, K.; Hayashi, T. Antiviral and Immunostimulating Effects of Lignin-Carbohydrate-Protein Complexes from *Pimpinella Anisum*. *Biosci., Biotechnol., Biochem.* **2011**, *75*, 459−465.
(30) Gordts, S. C.; Férir, G.; D'huys, T.; Petrova, M. I.; Lebeer, S.; Snoeck, R.; Andrei, G.; Schols, D. The Low-Cost Compound Lignosulfonic Acid (LA) Exhibits Broad-Spectrum Anti-HIV and Anti-HSV Activity and Has Potential for Microbicidal Applications. *PLoS One* **2015**, *10*, No. e0131219.
(31) Upton, B. M.; Kasko, A. M. Strategies for the Conversion of Lignin to High-Value Polymeric Materials: Review and Perspective. *Chem. Rev.* **2016**, *116*, 2275−2306.
(32) Sadeghifar, H.; Ragauskas, A. Lignin as a UV Light Blocker—A Review. *Polymers* **2020**, *12*, No. 1134.
(33) Tao, J.; Li, S.; Ye, F.; Zhou, Y.; Lei, L.; Zhao, G. Lignin − An Underutilized, Renewable and Valuable Material for Food Industry. *Crit. Rev. Food Sci. Nutr.* **2020**, *60*, 2011−2033.
(34) Sander, W. J.; Fourie, C.; Sabiu, S.; O'Neill, F. H.; Pohl, C. H.; O'Neill, H. G. Reactive Oxygen Species as Potential Antiviral Targets. *Rev. Med. Virol.* **2022**, *32*, No. e2240.
(35) Patil, S. V.; Argyropoulos, D. S. Stable Organic Radicals in Lignin: A Review. *ChemSusChem* **2017**, *10*, 3284−3303.
(36) Miglbauer, E.; Gryszel, M.; Głowacki, E. D. Photochemical Evolution of Hydrogen Peroxide on Lignins. *Green Chem.* **2020**, *22*, 673−677.
(37) Pica, N.; Langlois, R. A.; Krammer, F.; Margine, I.; Palese, P. NS1-Truncated Live Attenuated Virus Vaccine Provides Robust Protection to Aged Mice from Viral Challenge. *J. Virol.* **2012**, *86*, 10293−10301.
(38) Bertella, S.; Luterbacher, J. S. Simultaneous Extraction and Controlled Chemical Functionalization of Hardwood Lignin for Improved Phenolation. *Green Chem.* **2021**, *23*, 3459−3467.
(39) Rinaldi, R.; Jastrzebski, R.; Clough, M. T.; Ralph, J.; Kennema, M.; Bruijnincx, P. C. A.; Weckhuysen, B. M. Paving the Way for Lignin Valorisation: Recent Advances in Bioengineering, Biorefining and Catalysis. *Angew. Chem., Int. Ed.* **2016**, *55*, 8164−8215.
(40) Shuai, L.; Amiri, M. T.; Questell-Santiago, Y. M.; Héroguel, F.; Li, Y.; Kim, H.; Meilan, R.; Chapple, C.; Ralph, J.; Luterbacher, J. S. Formaldehyde Stabilization Facilitates Lignin Monomer Production during Biomass Depolymerization. *Science* **2016**, *354*, 329−333.
(41) Liao, J. J.; Latif, N. H. A.; Trache, D.; Brosse, N.; Hussin, M. H. Current Advancement on the Isolation, Characterization and Application of Lignin. *Int. J. Biol. Macromol.* **2020**, *162*, 985−1024.
(42) Bertella, S.; Luterbacher, J. S. Lignin Functionalization for the Production of Novel Materials. *Trends Chem.* **2020**, *2*, 440−453.
(43) ISO 21702: Measurement of Antiviral Activity on Plastics and Other Non-Porous Surfaces. *ISO 21702: Measurement of Antiviral Activity on Plastics and Other Non-Porous Surfaces*, 2019.
(44) Butot, S.; Baert, L.; Zuber, S. Assessment of Antiviral Coatings for High-Touch Surfaces by Using Human Coronaviruses HCoV-229E and SARS-CoV-2. *Appl. Environ. Microbiol.* **2021**, *87*, No. e01098-21.
(45) Haldar, J.; Weight, A. K.; Klibanov, A. M. Preparation, Application and Testing of Permanent Antibacterial and Antiviral Coatings. *Nat. Protoc.* **2007**, *2*, 2412−2417.
(46) Firquet, S.; Beaujard, S.; Lobert, P.-E.; Sané, F.; Caloone, D.; Izard, D.; Hober, D. Survival of Enveloped and Non-Enveloped Viruses on Inanimate Surfaces. *Microbes Environ.* **2015**, *30*, 140−144.
(47) Roques, S. C.; Landrault, N.; Teissèdre, P.-L.; Laurent, C.; BesanÇon, P.; Rouanet, J.-M.; Caporiccio, B. Hydrogen Peroxide Generation in Caco-2 Cell Culture Medium by Addition of Phenolic Compounds: Effect of Ascorbic Acid. *Free Radical Res.* **2002**, *36*, 593−599.
(48) Akram, N. A.; Shafiq, F.; Ashraf, M. Ascorbic Acid-A Potential Oxidant Scavenger and Its Role in Plant Development and Abiotic Stress Tolerance. *Front. Plant Sci.* **2017**, *8*, No. 613.
(49) Lanzalunga, O.; Bietti, M. Photo- and Radiation Chemical Induced Degradation of Lignin Model Compounds. *J. Photochem. Photobiol., B* **2000**, *56*, 85−108.
(50) Mileto, D.; Mancon, A.; Staurenghi, F.; Rizzo, A.; Econdi, S.; Gismondo, M. R.; Guidotti, M. Inactivation of SARS-CoV-2 in the Liquid Phase: Are Aqueous Hydrogen Peroxide and Sodium Percarbonate Efficient Decontamination Agents. *ACS Chem. Health Saf.* **2021**, *28*, 260−267.
(51) Urushidani, M.; Kawayoshi, A.; Kotaki, T.; Saeki, K.; Mori, Y.; Kameoka, M. Inactivation of SARS-CoV-2 and Influenza A Virus by Spraying Hypochlorous Acid Solution and Hydrogen Peroxide

Solution in the Form of Dry Fog. *bioRxiv* **2021**, DOI: 10.1101/2021.12.13.472413.
(52) Bidra, A. S.; Pelletier, J. S.; Westover, J. B.; Frank, S.; Brown, S. M.; Tessema, B. Comparison of In Vitro Inactivation of SARS CoV-2 with Hydrogen Peroxide and Povidone-Iodine Oral Antiseptic Rinses. *J. Prosthodontics* **2020**, *29*, 599−603.
(53) Meister, T. L.; Brüggemann, Y.; Todt, D.; Conzelmann, C.; Müller, J. A.; Groß, R.; Münch, J.; Krawczyk, A.; Steinmann, J.; Steinmann, J.; Pfaender, S.; Steinmann, E. Virucidal Efficacy of Different Oral Rinses Against Severe Acute Respiratory Syndrome Coronavirus 2. *J. Infect. Dis.* **2020**, *222*, 1289−1292.
(54) Kampf, G.; Todt, D.; Pfaender, S.; Steinmann, E. Persistence of Coronaviruses on Inanimate Surfaces and Their Inactivation with Biocidal Agents. *J. Hosp. Infect.* **2020**, *104*, 246−251.
(55) Conzelmann, C.; Weil, T.; Groß, R.; Jungke, P.; Frank, B.; Eggers, M.; Müller, J. A.; Münch, J. Antiviral Activity of Plant Juices and Green Tea against SARS-CoV-2 and Influenza Virus in Vitro. *bioRxiv* **2020**, DOI: 10.1101/2020.10.30.360545.

https://doi.org/10.1021/acssuschemeng.2c04284
ACS Sustainable Chem. Eng. 2022, 10, 14001−14010